

A COMPLETE EXPERIMENTAL INVESTIGATION OF GUST LOAD: FROM GENERATION TO ACTIVE CONTROL

Arnaud Lepage¹, Yannick Amosse¹, Dominique Le Bihan¹,
Charles Poussot-Vassal², Vincent Brion³ and Eric Rantet⁴

¹²³ ONERA - The French Aerospace Lab

¹ Aeroelasticity and Structural Dynamics Department, Châtillon, France, 92320

² Systems Control and Flight Dynamics Department, Toulouse, France, 31000

³ Fundamental and Experimental Aerodynamics Department, Meudon, France, 92190

⁴ AVIATION DESIGN, 38 ZI Le Chenet, Milly La Forêt, France, 91490

arnaud.lepage@onera.fr

Keywords: wind tunnel, gust load, aeroelasticity, closed-loop, active alleviation.

Abstract: In order to make substantial progress in reducing the environmental impact of aircraft, one of the key technologies investigated in the framework of the platform SFWA-ITD is the reduction of aircraft weight. This challenge requires the development and the assessment of new technologies and methodologies for both structural design and load control. To achieve the investigation of the specific case of gust load, ONERA had defined a dedicated experimental research program based on three Wind Tunnel Test (WTT) campaigns.

To reach these objectives, a new experimental set-up was designed and manufactured through an Aviation Design – ONERA collaboration and is composed of two main components implemented within the ONERA S3Ch transonic Wind Tunnel Facility. The first component, called gust generator, consists of two oscillating airfoils installed upstream of the wind tunnel test section and allows to produce air flow deflections. The second component, the test model, is a 2D supercritical airfoil equipped with a control surface and is based on the well-known 2 degrees-of-freedom (DOF) aeroelastic model (pitch and plunge motions).

A first WTT campaign has been carried out to qualify the unsteady flow induced by the gust generator and the ability to generate cylindrical gust field with significant and reproducible amplitudes in subsonic and transonic ranges. The second WTT was devoted to analyse gust effects on the test model behaviour for different structural and aerodynamic conditions. The aeroelastic model behaviour has been therefore characterized in terms of unsteady pressure and structural acceleration fields for both gust perturbations and control surface commands. These results provided the input data for the final WTT aiming at demonstrating the active gust load alleviation thanks to closed-loop control approaches. Real time feedback controls were tested during this WTT up to transonic conditions and have demonstrated significant reductions of the model structural responses to gust.

This work has been undertaken within the Joint Technology Initiative “JTI CleanSky”, Smart Fixed Wing Aircraft Integrated Technology Demonstrator “SFWA-ITD” project (contract N° CSJU-GAM-SFWA-2008-001) financed by the 7th Framework programme of the European Commission.

1 INTRODUCTION

1.1 The context project

Clean Sky is one of the largest European research programme ever launched in Europe. Its mission is to develop breakthrough technologies to significantly increase the environmental performances of airplanes and air transport [1]. The introduction of green technology into aviation is essential to make major steps towards the environmental goals sets by ACARE (Advisory Council for Aeronautics Research in Europe) to be reached in 2020:

- 50% reduction of CO₂ emissions through drastic reduction of fuel consumption
- 80% reduction of NO_x (nitrogen oxide) emissions
- 50% reduction of external noise

The purpose of SFWA ITD (Smart Fixed Wing Aircraft Integrated Technology Demonstrator) is to take innovative technologies of flow and load control to provide a step change in fuel consumption levels. The main improvements axes are the drag reduction using wing laminarity and aircraft weight reduction through novel load control technologies.

In this context, as part of the Technology Stream “Load Control Functions and Architectures”, ONERA intends to deal with the gust load case, which is one of the most critical for strength design and fatigue loading source for transport type aircraft. In academic or industrial research area, there are few works conducted on the experimental investigation of gust in wind tunnel, especially for the transonic regime. Studies have been performed in low speed regime based on various mechanisms for creating an oscillating flow in a wind tunnel: experiments based on rotating slotted cylinder [2] or composed of oscillating airfoils [3]. In the transonic speed range, very few wind tunnel experiments can be identified: concepts based on oscillating vanes [4] or using a single pitching airfoil [5] have been recently built in transonic wind tunnel environments. But considering these studies, there still is a lot of work to perform in order to improve the understanding of the physical phenomena involved in fluid structure interaction with a gust perturbation and therefore to improve the definition of gust load alleviation strategies.

To achieve the experimental investigation, ONERA proposed to define a research tool for the investigation of gust load in Wind Tunnel (WT) tests conditions. The key objectives for ONERA are :

- to improve the understanding of a large scope of physical phenomena induced by gust such as linear and non-linear aerodynamic in presence of gust, aeroelastic effects of an impact gust on a flexible model ...
- to dispose of comprehensive and relevant experimental databases for the validation of methodologies and tools of numerical simulation such as high fidelity tools of Computational Fluid Dynamic (CFD) and Computational Structure Mechanics (CSM) - such as the aeroelastic module of the ONERA software elsA [9].
- to investigate gust load alleviation with control approaches based on closed-loop architecture.

This paper will provide descriptions of all testing apparatus including the gust generation device and the aeroelastic model. Gust generator characterisation as well as open-loop testing will be presented. Finally the control methodology and the closed-loop testing procedures will be described.

1.2 ONERA experimental roadmap for gust load investigation

To achieve the objective, several wind tunnel tests (WTT) were achieved in the research ONERA S3Ch Wind Tunnel located in the ONERA Meudon Center [6]. This closed return wind tunnel is a transonic continuous run facility with a 0.8m x 0.8 m square test section for a 2.2m length. It covers a Mach range from 0.3 to 1.2 and operates at atmospheric stagnation pressure and stagnation temperature of approximately 310K. The top and bottom walls of the test section can be either rigid walls or deformable adaptive walls. In the latter case, the walls displacements are estimated in order to adapt the steady flow in the model area by minimising the wall interferences.

In this project, the experimental research means consist of two main parts implemented within the WT facility. The first part is dedicated to the generation of the gust field and is called “the gust generator”. The second is the model part which aerodynamic and aeroelastic behaviours were studied in presence of gust type perturbations. A schematic overview of the experimental test set-up is shown in Figure 1. The experimental set-up was designed and manufactured through an ONERA – Aviation Design collaboration, Aviation Design being a French S.M.E. winner of a Call for Proposal (SFWA Batch#7 – Acronym : Windtunnel [7]).

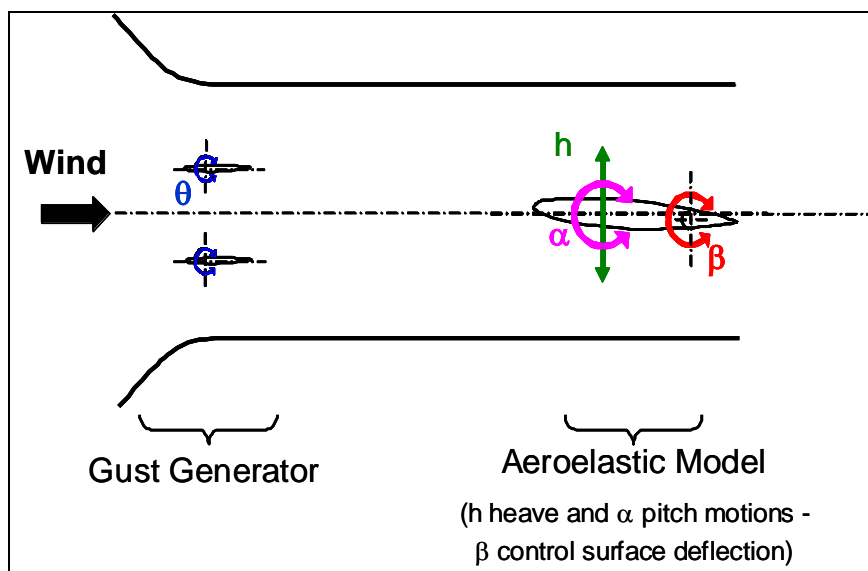


Figure 1: Schematic overview of the experimental test set-up

The experimental roadmap was defined with an increasing complexity with intermediate milestones. Three main Wind Tunnel Testing campaigns were scheduled:

- The first WTT was realised in order to qualify the gust generator characteristics and performances.
- The main objective of the second WTT was to acquire an experimental open-loop database and to analyse the effects of impacting gusts on a model behaviour.
- In the third WTT, the demonstration of the active gust load alleviation on a flexible structure was performed in real time conditions.

2 GENERATION OF GUST IN A TRANSONIC WIND TUNNEL

2.1.1 The gust generator

Dealing with gust in WT environment is always a challenging problem especially when the tests cover the transonic range. A basic solution to this problem is to install a gust vane device right at the beginning of the wind tunnel test section. The selected concept of the gust generator is composed of two movable 2D wings fixed on the walls of the wind tunnel. The geometric definition of the gust generator was based on preliminaries CFD simulations (URANS) using the elsA software. Parametric studies have been realised to investigate the influence of various parameters on the performances in terms of gust generation such as geometric parameters (airfoil type, chord, vertical and longitudinal position of wings), actuating parameters (frequency and amplitude of the pitch motion), aerodynamic conditions, interactions with the WT walls. Based on general trends of this numerical process, the geometrical architecture has been frozen: the gust generator is made of two identical NACA 0012 airfoils of $c = 0.2\text{m}$ chord length placed at $x = -0.63\text{m}$, upstream of the entrance of the test section which corresponds to $x = 0$, and at $h = \pm 0.2\text{m}$ above and below the wind tunnel longitudinal axis. The airfoils span covers the entire width of the tunnel with a minimal gap between the wing tip and the WT walls. An overview of this experimental set-up installed in the S3ch WT is shown in figure 2.



Figure 2: The experimental set-up of the first Wind Tunnel Test: the gust generator (foreground) and the unsteady clinometric probe (background)

The actuation is performed by four servohydraulic jacks which synchronously rotate the two airfoils (i.e. pitch dynamic motions about the quarter chord point). Each airfoil is driven at its two sides and the actuation device includes a security system that stops the actuation whenever the two roots of one airfoil are not at the same angular position, thus preventing any unwanted torsional deformation of the airfoils.

The 2 airfoils are made of an optimized architecture that combines carbon reinforced skins and metallic parts to reduce inertia and allow high frequencies of actuation under heavy aerodynamic loads. In addition to inertial and strength constraints, the dynamic behaviour of the airfoils was tuned such that the frequency of the first flexible structural mode is higher than the frequency bandwidth of the gust generator, i.e. 100Hz.

Preliminary to the wind tunnel tests, the complete experimental setup was qualified under laboratory conditions to identify the static and dynamic behaviours of each airfoil and to verify the performances of the actuation in pitch. In particular dynamic tests results were used in an aeroelastic calculation procedure to ensure the absence of any instability (flutter, static divergence) in the range of the wind tunnel test conditions. The airfoils were equipped with several accelerometers, pressure transducers and deformation gauges.

2.1.2 Measurement devices during the first WTT

The first campaign in the S3Ch WT started at the end of 2012. The goal of these experiments was to estimate whether the gust generator was able to generate a relevant gust field and to qualify its characteristics. Two measurement devices were used to qualify the flow :

- An unsteady clinometric probe especially designed and manufactured for these tests. This “gust sensor”, visible in the background of the figure 2, is a fast-response 2 holes probe equipped with 2 unsteady pressure sensors. Before the first WTT, the probe was calibrated in situ, i.e. in the test section, by measuring the pressure difference between the 2 sensors at prescribed flow incidences and for a steady incoming flow. As expected, the calibration law is established by the following relation $\alpha = a \cdot \Delta P / Q_0 + b$ with α the flow angle, ΔP the pressure difference between the 2 sensors and Q_0 the upstream dynamic pressure. The post processing of probe data indicated a small dispersion in Mach number of the “a” proportional term contrary to the “b” term traducing the natural incidence at the measurement point in the WTT section.
- A two components phase averaged Particle Image Velocimetry (PIV) system. The device is composed of a double pulse laser and a high resolution camera. The laser was installed below the test section and delivered an (Oxz) measurement plan. The time resolution was obtained through phase averaging locked to the airfoil motion which period was decomposed into N phases. More details on the measurement process and the data post processing can be found in [8].

2.1.3 Typical results of the gust generator performances

The functioning of the gust generator during the wind tunnel tests met the requirements and the specifications fixed at the beginning of the project. The dynamic actuation of the 2 wings performed during laboratory tests was reproduced during WTT with a quasi-perfect synchronism of the four actuators. The results and analyses indicated that this gust generator allowed to generate a cylindrical gust field in wind tunnel environment in a reproducible way with significant gust amplitudes.

Typical results are shown in Figure 3 presenting temporal evolutions of the "gust signal" for a harmonic oscillation of the gust generator. As expected, a sinusoidal command induced a sinusoidal dynamic motion of the 2 wings generating therefore a sinusoidal gust. For this example for Mach number of 0.3 (respectively 0.73), a dynamic actuation of the wings of $\pm 5^\circ$ in amplitude at 20Hz (respectively $\pm 2^\circ$ at 40Hz) induced a gust amplitude recorded by the probe of about $\pm 0.8^\circ$ flow deviations (respectively $\pm 0.37^\circ$). A frequency analysis of the gust signal is also given in Figure 3. The principal component of the gust field is located on the command frequency. Higher harmonics could be identified but with a lower order of magnitude.

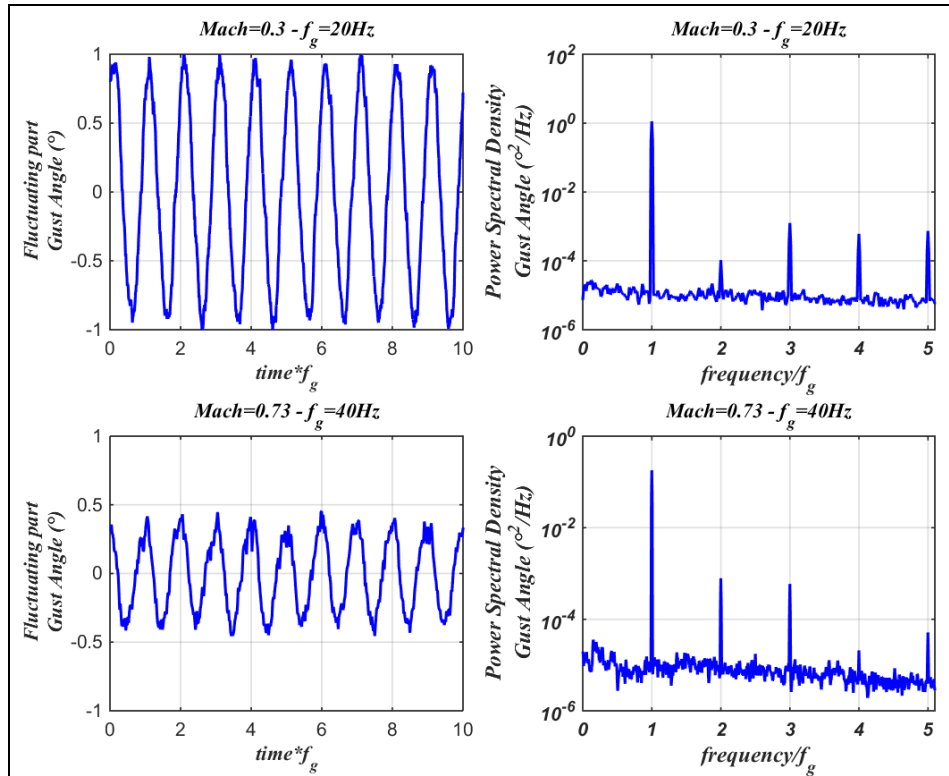


Figure 3: Signals obtained by the unsteady clinometric probe and associated spectra for Mach 0.3 and 0.73 and a frequency generation of 20 and 40 Hz at X=1.2m and Z=0m

In addition to probe data, PIV measurements have allowed to qualify complementary the unsteady flow of the gust field. Figure 4 shows the spatio-temporal reconstructions of the longitudinal and vertical velocity components for the similar tests point presented in figure 3. Each frame represents the flow variations over one wavelength of the gust.

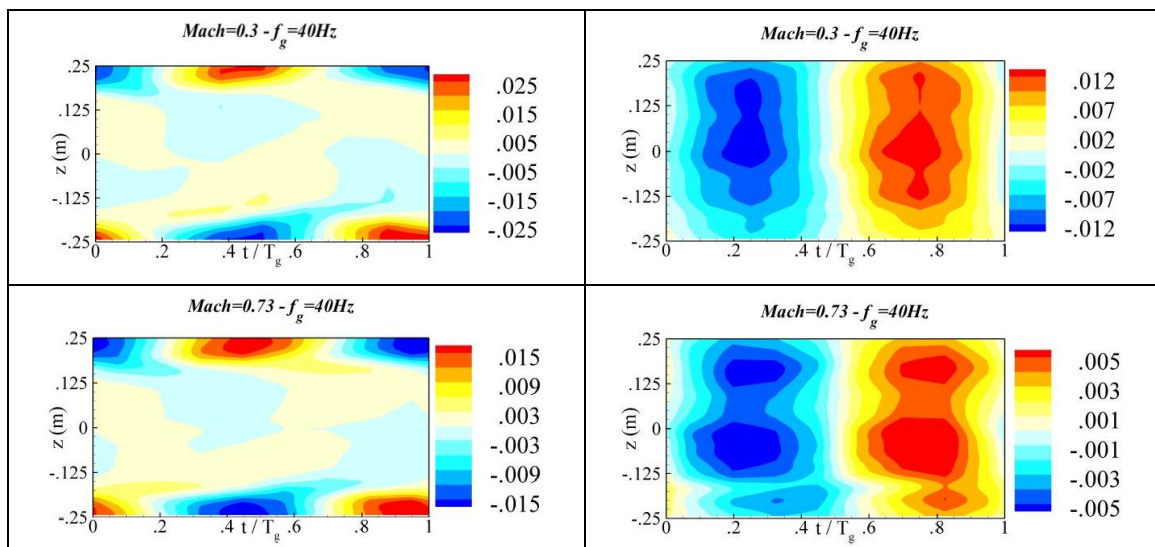


Figure 4: Normalised longitudinal (U/U_∞ - left) and vertical (W/U_∞ - right) velocities obtained by PIV for Mach 0.3 and 0.73 and a frequency generation of $f_g=40$ Hz – Time line normalised by the gust period $T_g=1/f_g$ – Spatial measurements at X = 1.2m (probe location)

The influence of the walls and the effects of the wings wake ($Z=\pm 0.2m$) are clearly emphasized with strong variations of the velocity longitudinal components while small scale

disturbance are observed in central area ($Z \sim 0m$). The vertical velocity field demonstrates clearly an alternating upward and downward flow, i.e. an alternating positive and negative flow angle, as function of time which exactly corresponds to the researched phenomenon. The analysis along the vertical axis indicates a variation of homogeneity which is still nevertheless moderated in the center area.

2.1.4 Main outcomes of the qualification of the gust generator

The first WTT was performed following a parametric approach: the gust field properties were analysed depending on the aerodynamic conditions and the actuating conditions. Significant parameters have been investigated:

- The amplitude of the dynamic actuation which appears to be a quasi linear parameter in terms of generated gust amplitude. Moreover significant amplitude of actuation improved the signal to noise ratio, i.e. the gust components are more highlighted from the turbulence natural noise of the wind tunnel.
- The frequency of the dynamic actuation which drives obviously the wavelength of the generated phenomena through the well-known relation $\lambda = U_\infty / f$. Moreover, the frequency parameter has a linear effect on the resulting gust amplitude.
- The velocity U_∞ of the flow which drives directly the gust amplitude through the velocity ratio V_z / V_x .

The Figure 5 summarizes the main characteristics for the case of harmonic gust. The gust amplitude α_{Gust} is normalised on the actuation amplitude $\alpha_{Actuation}$ and a correction factor $\beta = 1 / (1 - M^2)^{1/2}$ of the compressibility effects (according to the Prandtl-Glauert transformation). The resulting normalised gust angle is plotted versus the reduced frequency $k = 2\pi f * c / U_\infty$, c being the chord of the gust generator wings.

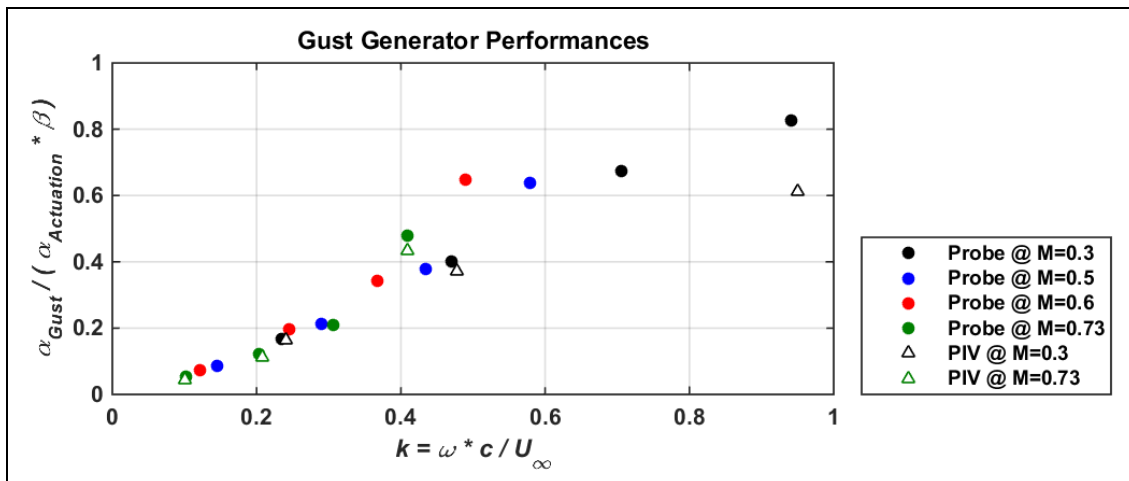


Figure 5: Synthesis of the performances of the Gust Generator

The figure 5 indicates clearly a good correlation between the probe and PIV measurements. Moreover these data are in a good agreement with numerical predictions and analytical models developed in [8]. The main outcomes indicate that the reduced frequency k and the dynamic pitch amplitude $\alpha_{Actuation}$ are the dominant parameters with a positive effect on the gust generation. The Mach has also a beneficial effect in lower order of magnitude by improving the airfoil performances. This typical chart presented in figure 5 has been used

as inputs data (i.e. “gust abacus”) for the following WTT in order to define the gust load perturbation impacting the aeroelastic model.

The analyses of WTT1 databases led to the conclusion that the gust generators fully filled the requirements and specifications. The gust generation process is controlled and sufficient to induce aerodynamic and aeroelastic effects on the model.

3 WIND TUNNEL AEROELASTIC MODEL

3.1 Aerodynamic considerations of the model

As for the gust generation device, the model was designed and manufactured by Aviation Design. The model consisted of a 2D airfoil mounted between the walls of WT sections with specific boundary conditions allowing two flexible degrees of freedom (dof): pitch and plunge motions.

The airfoil is based on an ONERA supercritical profile (OAT15A) which design point is for a Mach number of 0.73 and a lift coefficient of 0.65 [10]. The thickness to chord ratio is 12.3%, regarding the WT dimensions, a 250 mm chord was chosen with a resulting 3.2 aspect ratio.

As the experimental database will be used for the validation of high fidelity numerical codes of CFD / CSM, a great attention was placed to respect the aerodynamic shape of the airfoil.

A specific manufacturing process was defined by Aviation Design in order to avoid any geometrical variations due to molds defaults and temperature effects. The main components of the airfoil part are composed of a steel spar and 2 upper and lower carbon reinforced skins.

The design of the model was performed without any cover or access on each sides of the wing. Consequently, the whole model instrumentation was realized simultaneously with the manufacturing.

3.2 The aeroelastic part of the model

The aeroelastic model aims at representing the behaviour of a classical 2 dof aeroelastic model that can be found in the literature, .i.e. a 2D model with a pitch and plunge stiffnesses [11]. Common plunge-pitch model design approaches are reported in the state of the art and are devoted most of the time to flutter phenomena purposes. One of the most well-known is the Pitch And Plunge Apparatus (PAPA) developed at NASA [12] providing the two flexible dof needed for classical flutter. This device consists of a fixed plate attached to the tunnel sidewall turntable, a set of fixed-end rods and a moving plate. Contrary to these approaches, in the presented works, the choice of a 2D model was very specific and led to the definition of a symmetrical mounting part, and very few studies referred to this case.

Therefore a novel concept has been studied for the design of a pitch-plunge device. The stiffness properties are driven by flexible beams with in addition an arrangement of bearings in order to better “constrain/prescribe” the (“rigid body”) motions of the wing. A global overview of this mount is shown in figure 6. The solution is well adapted to the ONERA S3Ch WT environment, small and compact and requires no modifications of the WT.

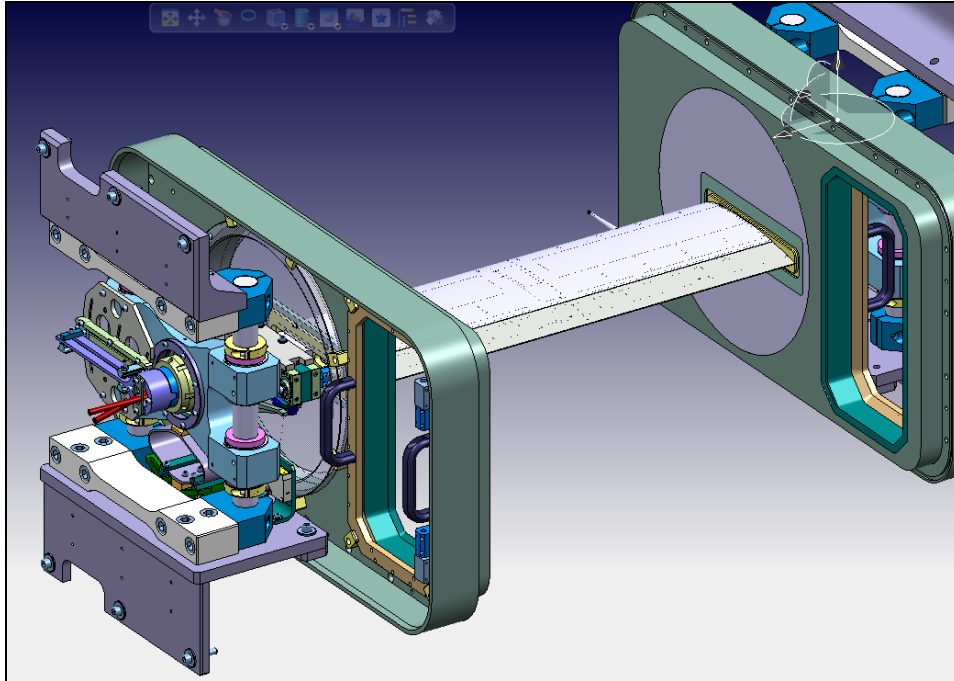


Figure 6: Overview of the 2D aeroelastic model installed in the S3 WTT section

For both dof, the geometrical parameters of stiffness beams (i.e. cross sections parameters, length and material characteristics) have been numerically optimized through Finite Element Models (FEM) in order to satisfy static loads requirements and to tune dynamics properties in the frequency range of interest. The main advantage of this mount system is that pitch and plunge stiffnesses can be modified independently by adjusting the length of clamping condition of each “stiffness beam”. This interesting feature allows to study various structural configurations (from well-spaced frequencies to closed frequencies). Moreover, weights can be added to modify the modal frequencies and also to decouple the pitch and plunge modes by moving the center of gravity of the model forward or aft as necessary (to locate it on the system elastic axis).

In the wind-tunnel test section, the global 2dof mounting system is composed of 2 identical mountings parts located on each test section door. On both sides, the wing part is attached to the 2dof system at each wing root by a connection to the pitch shaft located at 30% of the chord. The device includes also mechanical stops to limit dynamic motions in case of too high oscillation amplitude. Moreover the pitching device allows to modify the wing model angle of attack (AoA) in a large range.

3.3 The control surface and the instrumentation of the model

As one of the main objectives of the experimental roadmap is to performed active gust load alleviation, the model needed to dispose of a control mean. The choice of a full span trailing edge control surface was made to preserve as much as possible the 2D behaviour of the flow. The hinge axis was located at 75% of the chord. On each side, the control surface is driven by a high torque - high speed actuator especially designed and manufactured for these tests – figure 7. Each actuation device is composed of a rotative hydraulic actuator operating at 200 bar using a fast response servo valve and a Rotary Variable Differential Transducer (RDVT). Actuation bandwidth is an important consideration for gust load alleviation law design and performance. Here the goal was to cover the wide frequency bandwidth achievable by the gust generator, i.e. up to about 100Hz. Position feedback control laws were precisely tuned to

allow the dynamic deflection of the control surface. Performances of the actuators were assessed by estimating the Frequency Response Function (FRF) of the rotation position relatively to command signal –figure 8. The synchronous dynamic functioning of the two actuators was validated in terms of phase and amplitude over the frequency bandwidth.

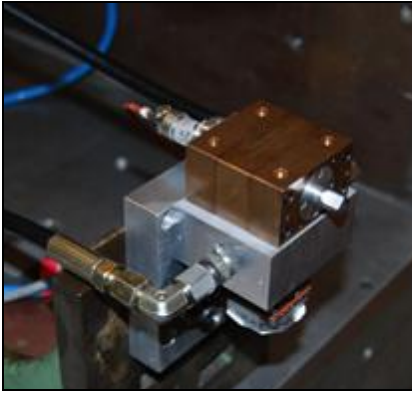


Figure 7: Overview of a high torque – high speed hydraulic actuator

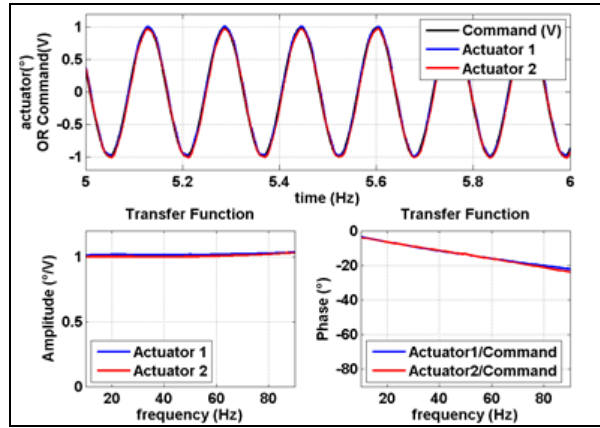


Figure 8: Typical temporal evolution of command and rotation signals and associated FRF

In order to generate an experimental database for the validation of high fidelity numerical codes, different measurements techniques were selected for the wind tunnel tests. The main part of the instrumentation is made of steady (31) and unsteady pressure (44) transducers arranged mainly in two span stations. Additionally the model is equipped with accelerometers mounted (12) in three span stations in order to correctly handle the dynamic motions for both flexible and rigid motions of the model parts. The main embedded instrumentation is synthetized in Figure 9. Various strain gages bridges were located in different flexible parts of model. The objective was to monitor, during the WT tests, the bending of the main spar, the “pitch stiffness” and the “plunge stiffness” beams. Following the same design as for the probe described in the section 2.1.2, a similar unsteady clinometric probe was manufactured. This “gust sensor” can be easily removed or mounted in the airfoil leading edge and allowed to estimate the gust field upstream the airfoil section.

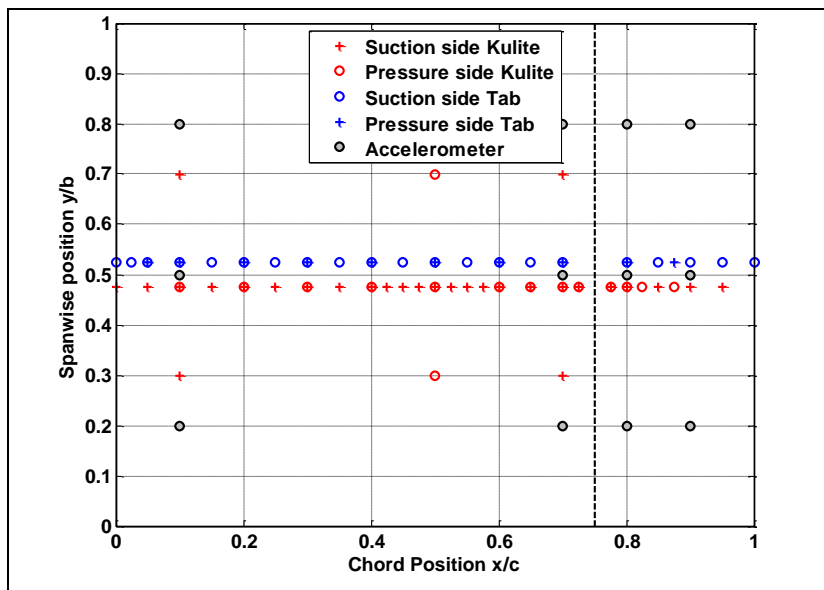


Figure 9: Locations of embedded pressure sensors and accelerometers

3.4 The model characterisation in laboratory conditions

Multiple tests were performed on the complete experimental set-up in the laboratory of the Department of Aeroelasticity and Structural Dynamics (DADS) at the Châtillon ONERA Center. A mechanical frame and a massive bracket were used to simulate the mounting conditions in the S3Ch WT. The first tasks were devoted to qualify the static behaviour of the model with static loads tests. Then the main step was the qualification of the dynamic behaviour with the main objective to estimate the structural parameters, i.e. modal parameters such as eigenfrequencies, modal dampings, modal masses and mode shapes. A classical methodology of experimental modal analysis was applied: the structural sensors responses were recorded using embedded and additional accelerometers relatively to different excitation signals and locations of dynamic shakers – figure 10.



Figure 10: Test set-up for the dynamic qualification

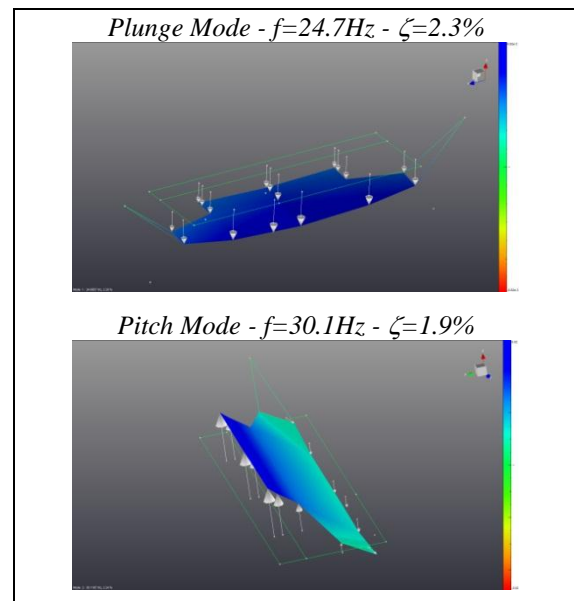


Figure 11: first two structural modes

During the dynamic tests, the main hard point was the presence of non-linearities in the structural behaviour of the model, especially for the plunge mode. During the design process, the use of bearing was chosen in order to prescribe the two dof. The resulting effect led to the apparition of friction phenomena and especially starting friction forces. Nevertheless, a fine analysis indicated that this non-linearity followed a classical behaviour: the modal frequency decreased with the level of energy but once a force level was reached, the frequency evolution followed an asymptotic behaviour with minor variations.

Regarding the modes order, the modal behaviour respected the model specifications: the two “rigid body” modes (i.e. the plunge and pitch modes) are present in low frequency (i.e. the low range of the useful bandwidth of the Gust Generator) while the first flexible mode (i.e. the bending mode) is located at higher frequency. Also positive from a technical perspective, the mode shapes were clean and uncoupled. In particular, the plunge and pitch mode shapes were mainly composed of rigid body components as expected – figure 11. Moreover, the designed 2 dof mount system allowed parametric variations of the modal frequencies depending on the clamping conditions of the “stiffness beams”.

The modal parameters were used in a flutter calculation procedure to ensure the absence of any aeroelastic instability. Parametric analyses were achieved for various clamping conditions and covering the envelope of the aerodynamic parameters of the WTT matrix.

4 OPEN-LOOP GUST LOAD TESTING

4.1 WTT conditions

The second campaign in the ONERA S3Ch Wind Tunnel started at the beginning of 2014. The goal of these experiments was to acquire the open-loop database i.e. the response of the aeroelastic model for an impacting gust. An overview of this experimental set-up is shown in Figure 12. In the background, the gust generator device is located in final part on the convergent area of the wind tunnel while the wing part of the aeroelastic model is visible downstream in the test section equipped with the adaptive walls.

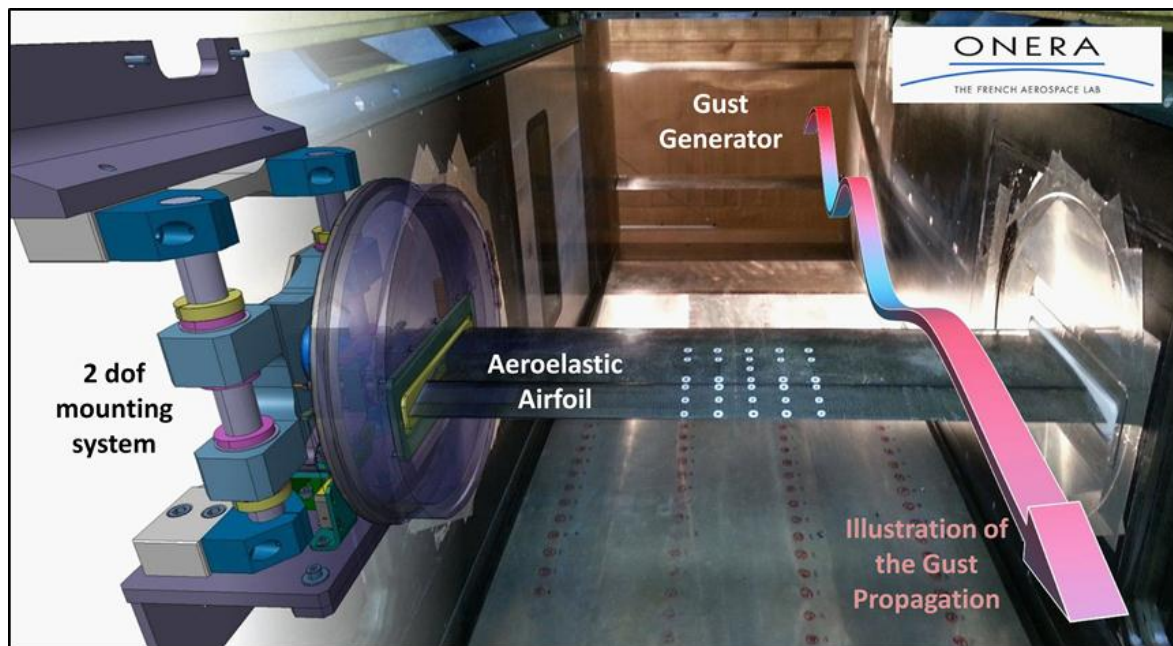


Figure 12: Experimental set-up of the second Wind Tunnel Test: the gust generator (background) and the aeroelastic model (foreground)

In order to correctly handle gust effects on the model, the test matrix was built to study different structural configurations (rigid vs flexible) and aerodynamic conditions. The objectives were to cover a wide range of physical phenomena from subsonic linear cases up to transonic non-linear cases.

4.2 Aerodynamic behaviour in presence of gust

The first part of the second WTT was devoted to the study of the aerodynamic phenomena induced by gust on the airfoil. To reach this objective, the clamping conditions of the model were switched in “rigid configuration” : the plunge beams were substituted by massive metallic parts while the clampings of the pitch beams were adjusted to postpone the mode at higher frequency.

The plots shown in Figure 13 to Figure 16 present the typical results of a sinusoidal gust impacting the airfoil at a transonic Mach. The analyses of the unsteady pressure sensors located on the Kulites chord are described. In Figure 13, the grey surface covers all instantaneous pressure distribution recorded at high sampling rate while red and blue lines provided the time averaged data. As shown, the pressure levels fluctuations were significant in the supersonic plateau area and the shock location. The pressure signals were modulated at

the Gust Generator frequency and for this case, the shock oscillated with a 8% chordwise amplitude between the extreme locations. The spatio-temporal representation described in Figure 14 emphasizes clearly the area of fluctuations induced by gust with extreme values near the shock location. Downstream the shock foot, the amplitudes of fluctuation are strongly attenuated with an inversion on the sign ($\Delta=180^\circ$ on the phase). The first harmonic pressure distribution exhibited a classical shape – figure 15. Contrary to subsonic case, pressure distribution is completely different between the suction and pressure sides. An important motion of the shock occurred and a shift on the phase information.

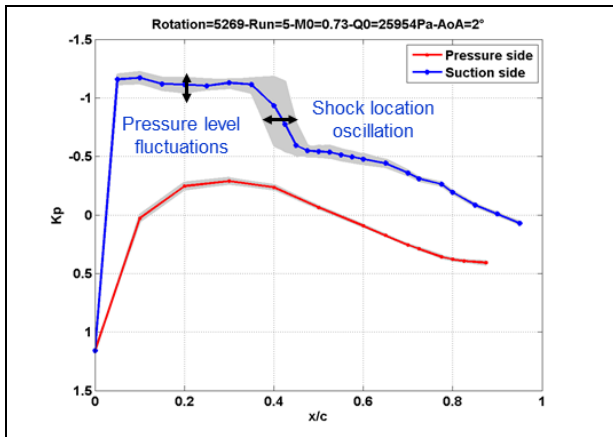


Figure 13: Instantaneous (grey) and averaged (blue and red) pressure coefficient distributions

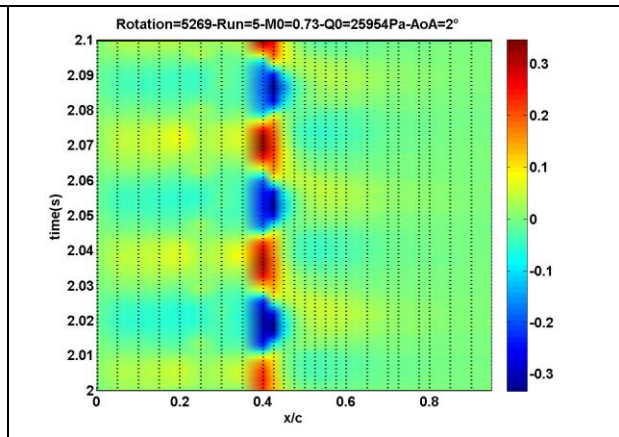


Figure 14: Spatio-temporal representation of pressure coefficient fluctuations $\Delta K_p(x,t)$

In order to estimate the global effects of impacting gusts on the aerodynamic behaviour of the airfoil, the unsteady lift force has been determined by integration of the unsteady pressure sensors, i.e. for each sample time. As shown in figure 16, the lift coefficient signal is obviously dominated by the frequency of the gust generator command. For the presented example, the order of magnitude of the local lift coefficient is $\Delta C_l = \pm 0.04$ leading to a variation of the lift force of about $\pm 200N$. This clearly demonstrates the ability of generating significant loads on the airfoil using the gust generator.

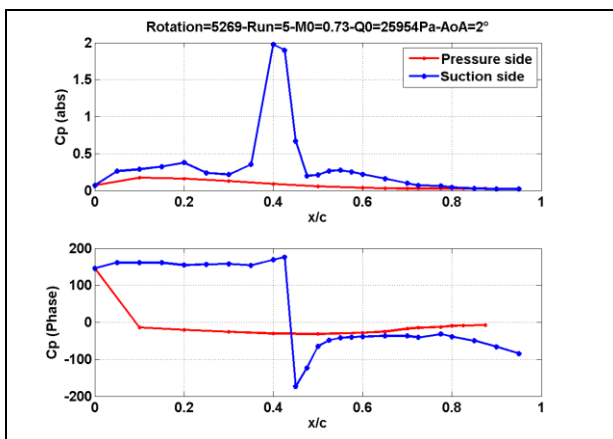


Figure 15: Distribution of First harmonic Pressure Distribution

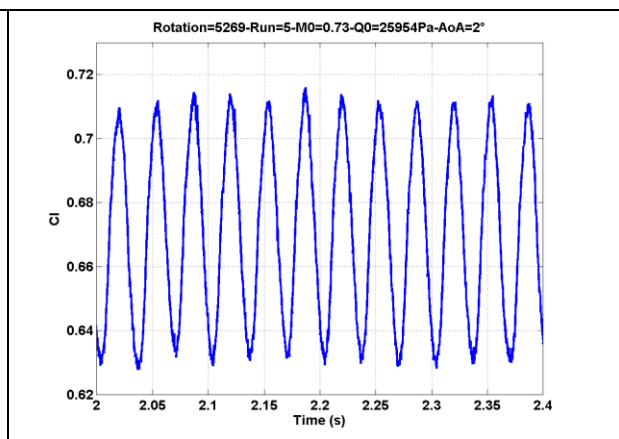


Figure 16: Temporal evolution of the lift coefficient signal obtained by pressure integration

4.3 Aeroelastic behaviour in presence of gust

For the aeroelastic part of the WTT program, the goal was the acquisition of the transfer function between the elastic wing motion and both the gust perturbation and the control surface command. The structural configuration was switched in “flexible case” with well-spaced modes, the plunge, pitch and first bending being located respectively at 25 Hz, 40 Hz and 72 Hz.

At each stable WT condition (Mach, α), sine sweep signals were used as input data. For the gust case, the signal amplitude was modulated as function of the time to compensate the frequency effect described in the section 2.1.4. in order to generate a constant amplitude gust over the wide frequency bandwidth. Figure 17 shows typical time histories and the associated FRF for Mach number of 0.73. The plunge and first bending modes can be seen in temporal signals of the wing accelerometers for a gust perturbation.

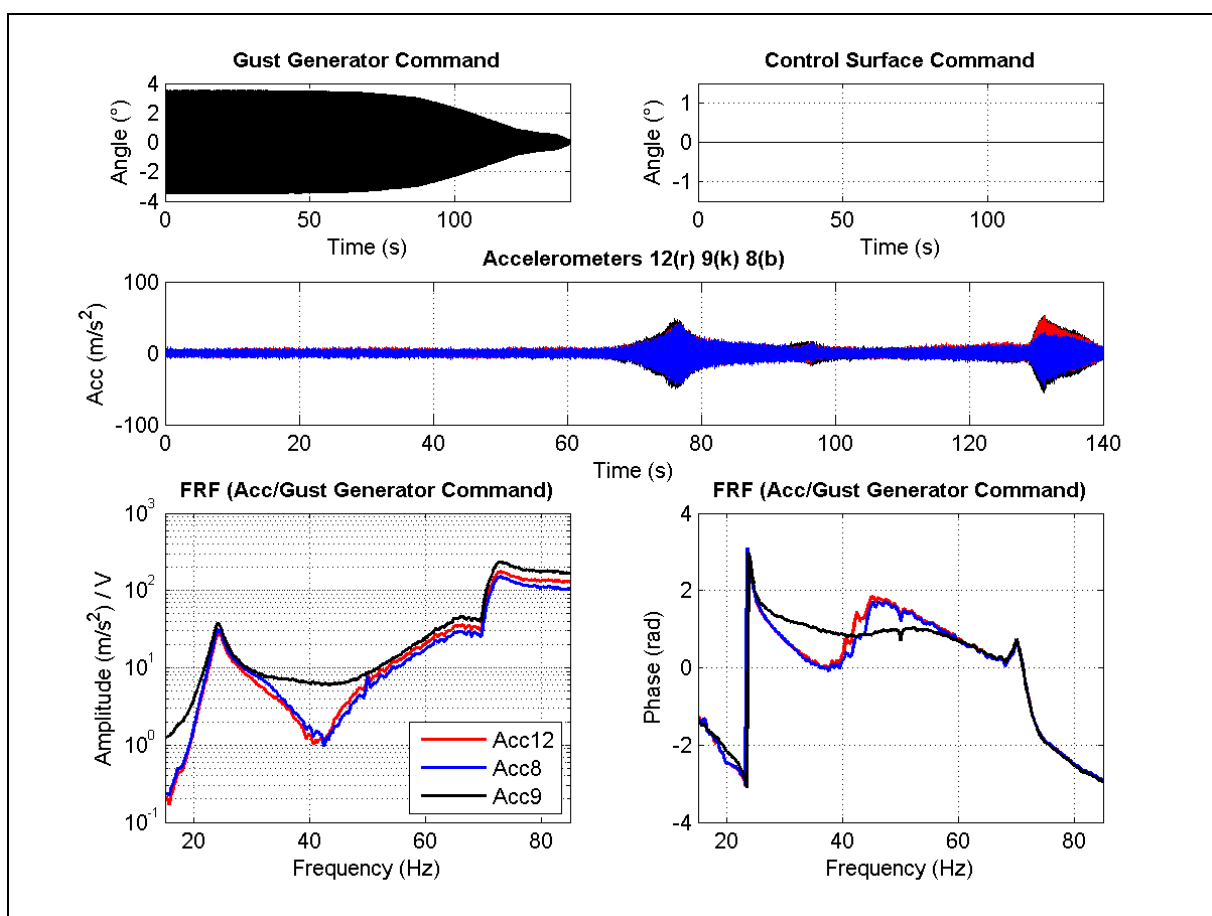


Figure 17: Time histories of gust command, control surface command and accelerometers and associated FRF – Gust generator command based on a sweep sine signal with an amplitude modulation – Tests at $M=0.73$ and $AoA=0^\circ$

Unfortunately, as presented in the FRF plots figure 17, the tests demonstrated that it was unexpectedly impossible to excite the pitch mode (around 40 Hz). Although its behaviour was clearly linear and controlled during lab tests, the gust perturbations didn't allowed to obtain significant responses on this mode. At the same time, as presented in figure 18, the pitch response clearly participated in the structural responses for a control surface input. Parametric analyses were performed to solve this issue and led to the conclusions of friction phenomena. During the design process, given that the expected airfoil dynamic motions, a specific attention was devoted the sealing problematic in the walls-airfoil junction. A sealing plate

made of anti-adhesive material was designed to ensure both sealing and motion, but the analyses have indicated remaining friction areas. This underestimated issue stills under investigation.

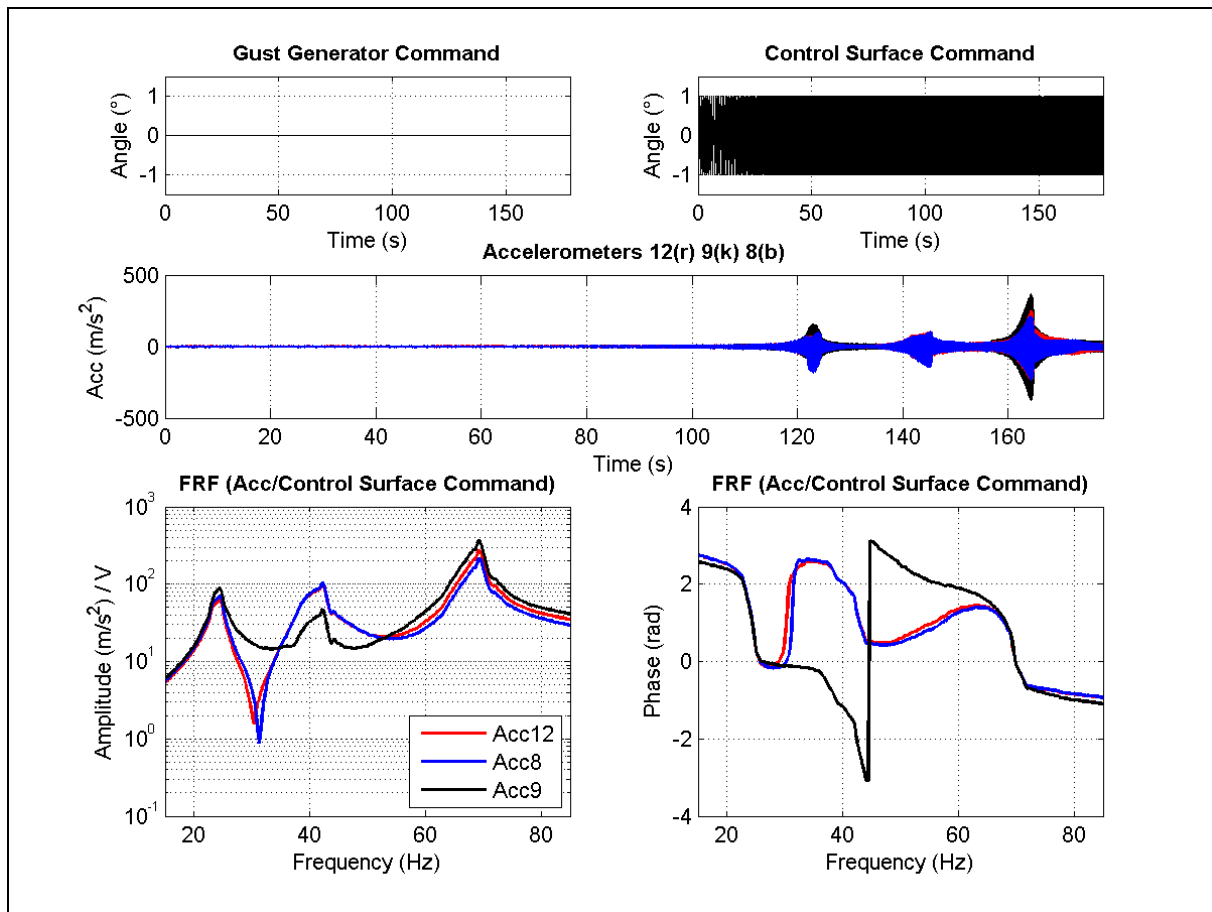


Figure 18: Time histories of gust command, control surface command and accelerometers and associated FRF – Control surface command based on a sweep sine signal – Tests at $M=0.73$ and $AoA=0^\circ$

On both temporal and frequency data plotted in figure 18, the three targeted modes (plunge, pitch and bending) are clearly visible, especially on the command transfer. In the view of achieving a closed-loop control, this point has guaranteed an a priori good controllability of these modes. The shape of the peak in the vicinity of the pitch frequency tends to indicate a non-linear behaviour. This confirms the previous assumption of friction phenomena associated to this structural mode.

5 GUST LOAD ALLEVIATION BY CLOSED-LOOP CONTROL

5.1 Control synthesis

Based on the experimental data (open-loop FRF), the plant dynamic behaviour was identified through the derivation of space state model for each WTT conditions (Mach, angle of attack).

Whatever the nature of the control problem (i.e. set point tracking or disturbance rejection), the achievement of control outcomes involves two main steps. The first is to describe using a closed-loop diagram incorporating the open-loop model (plant), the shape and structure of the loop to implement experimentally. Based on the robust synthesis tools, frequency weighting

filters are introduced in this diagram to act as constraints on the expected behaviour of representative quantities of the loop system.

After reformulation with the standardized Linear Fractional Transformation (LFT) form, the second step leads, using robust synthesis tools, to get controllers by minimizing the H_∞ norm of the singular values and FRF plots of the closed-loop system.

The augmented closed-loop is represented by the diagram of Figure 19-left : the noises of measurement and command signals d_m and d_u are white noises passed through W_{dm} and W_{du} filters. The W_p performance filter force the frequency band affecting the output sensitivity $S_y = (I+GK)^{-1}$ and W_u complementary input sensitivity $T_u : (I+GK)^{-1}GK$. The characteristics of the singular values of S_y adjust the efficiency bandwidth (i.e. the reactivity rate to the disturbance, the gain of disturbance rejection) and improve the robustness to parametric uncertainties (i.e. differences between the real structure and the identified model). T_u improves the high-frequency behaviour in terms of noise rejection and high frequency dynamic neglecting. The standard LFT form of the equivalent closed-loop system is shown on the right part of figure 19.

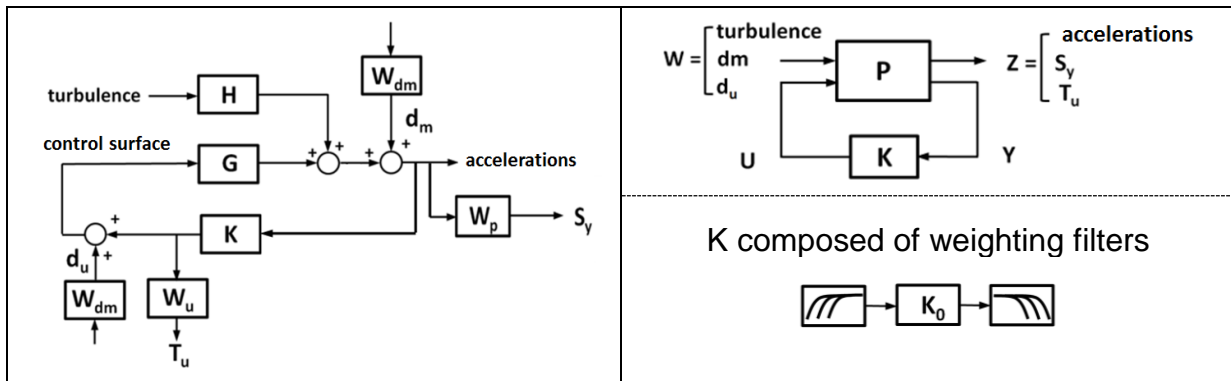


Figure 19: Mapping the control problem

The created state space model was directly used by the synthesis algorithms to calculate a stable and proper controller K such that the closed-loop T_{zw} is stable and $\|T_{zw}\|_\infty < \gamma$ positive scalar. The *hinfsstruct* function of the Robust Control Matlab Toolbox was mainly used as it allows more flexibility in configuring an initial controller (i.e. choice of the controller structure, parametric additional filters on Input/Output).

5.1.1 Controller implementation

The synthesized controllers were implemented on a real time dSpace device which was comprised of several processors and Input/Output boards interlinked for fast internal communication and data exchange. The I/O interface was composed of a maximum of 15 analog inputs and 18 analog outputs.

A dedicated computer was used for creating, compiling and implementing Simulink models in the processor boards and a real-time man/machine interface was developed to monitor the signals and change control/command parameters.

Synthesized in the continuous time domain, the controllers were converted into discrete state space models model to be directly implemented. With respect to the bandwidth of the electro-hydraulic actuator, a 2 kHz sampling frequency was selected and the real time device was associated with adapted anti-aliasing filters and smoothing filter on the command signal.

Several control architecture were tested and based on accelerometers data in a SISO configuration (i.e. Single Input Single Output) or MISO (i.e. Multi Input Single Output).

5.2 Closed-loop Control results

In the final WTT, the main objective was the demonstration in real time of gust load alleviation through the active control of the model aeroelastic response for a gust disturbance. For this first demonstration, the control laws were designed to act on the first plunge mode and to avoid any bad effect of the higher modes (e.g. amplification of the first bending).

Practically, the control parameter (controller, gain and loop sign) were tuned at first in real time for a harmonic gust perturbation with a sinusoidal command locked on the plunge mode frequency. An example of an accelerometer time history located in the central section is given in figure 20 for a test point $M=0.73$ and $AoA=0^\circ$. The left plot clearly demonstrates the control efficiency when the control is switched on. A quantitative evaluation for this test point pointed out a strong reduction of the model aeroelastic response up to -15 dB – right part of figure 20. The analysis of the control surface deflection indicated reasonable motions around one degree.

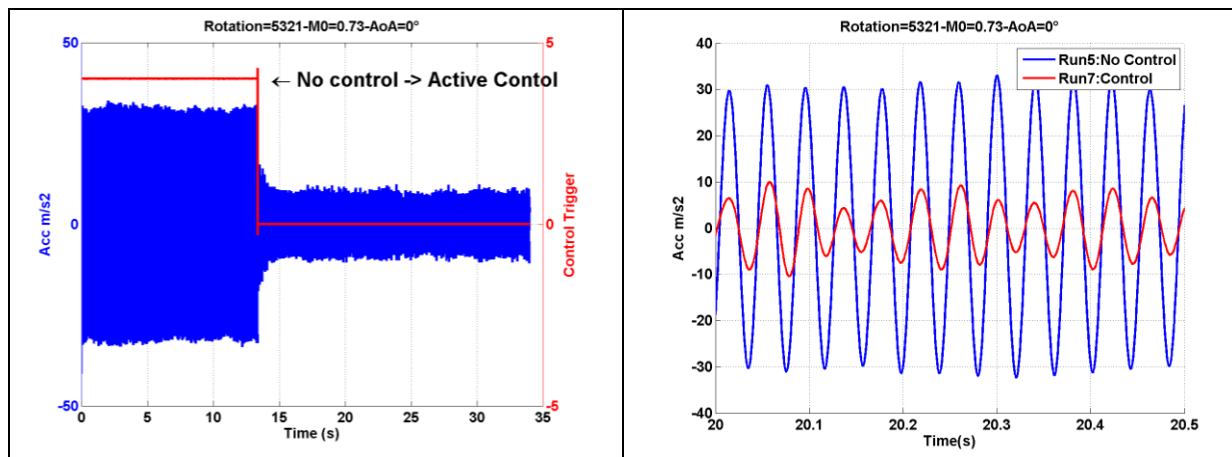


Figure 20: Accelerometer time history located at $x/c=0.1$ and $y/b=0.5$ for a sinusoidal gust perturbation at $f=24.5\text{Hz}$ in transonic flow $M=0.73$ and $AoA=0^\circ$

Then the control efficiency was assessed for a wide band gust excitation driven by a sweep sine command. Depending on the controller type and the test case, some margin could have been considered on the main feedback gain to ensure stability of the closed-loop system over the wide frequency bandwidth. Typical results are shown in figure 21 for subsonic and transonic cases. The open-loop data (i.e. without control) are superposed with the closed-loop data (with active control). As expected, the control laws are very efficient in vicinity of the plunge mode and no amplification appears at higher frequency. For the transonic case, structural responses attenuations up 70% were observed on the plunge mode and more for the subsonic range (around 80 %).

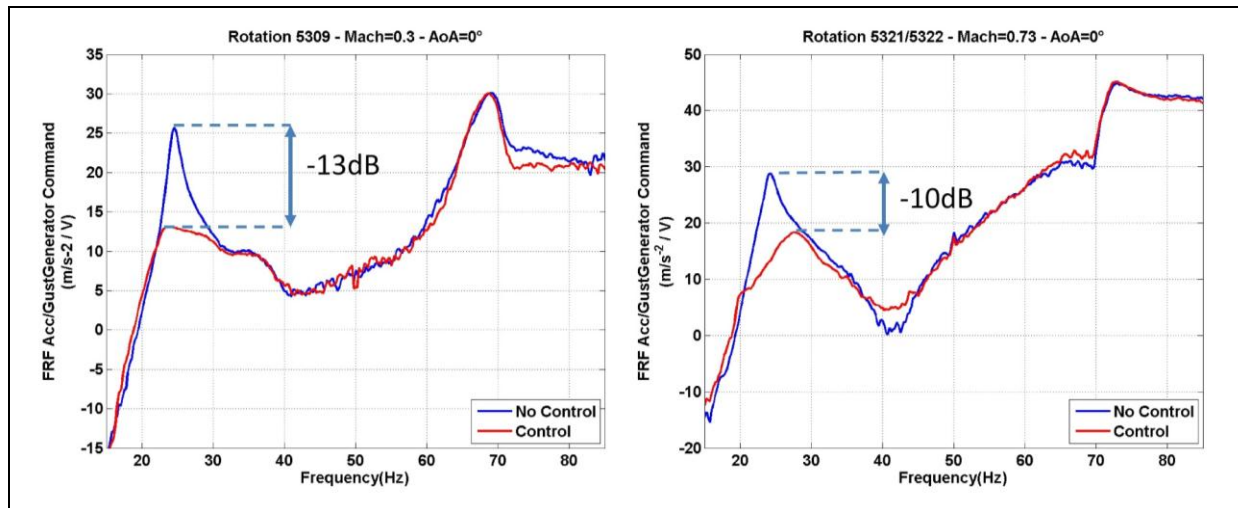


Figure 21: Demonstration of the active gust load alleviation .- FRF (amplitude - dB) between model accelerometer and the gust driving signal – Sweep sine gust perturbation – Tests at $M=0.3$ and 0.73 for $AoA=0^\circ$

Although the Ground Vibration Test (GVT) have demonstrated the presence of structural non-linearities, the robust control approach to take into account the effect of the parameter variations and uncertainties ensuring a control efficiency.

Moreover, at the end of the final WTT, the controller robustness was also characterized through parametric tests. Typically, a controller designed from a given open-loop dataset was tested with variations of the Mach number, the AoA value or the static angle of the control surface. The results have demonstrated structural response reductions in a lesser extent but also the absence of instabilities.

6 CONCLUSION

According the experimental roadmap, three WTT have been achieved in S3Ch in 2013 and 2014. The first has allowed to qualify efficiently and parametrically the gust generator capabilities relatively to different aerodynamic conditions. The database analyses have led to the conclusion that the gust generator fulfilled the requirements specifications: this device has allowed to generate a cylindrical gust field in wind tunnel environment in a reproducible and controlled way.

For the two last WTT, the experimental setup was well adapted regarding the specifications and the objectives and demonstrated its capacity to study unsteady aerodynamics and aeroelasticity in presence of gust. The achieved open-loop tests have provided a comprehensive and consistent database with parametric variations of the aerodynamic conditions, the gust perturbation properties and the control surface parameters. These data are currently used by the SFWA partners in a numerical restitution process to perform CFD/CSM simulations for gust cases. The users have pointed out the fact this database constitutes a major step in the validation process of the simulation capacities of gust, especially data acquired in the transonic ranges with non-linearities (flow separation).

Finally, active gust load alleviation was successfully demonstrated in real time up to transonic conditions. The control methodology was based on closed-loop architecture between accelerometers and the control surface command. The controller synthesis with the robust control approach provided various sets of control laws derived on experimental data (i.e. open-loop data). The closed-loop testing has demonstrated significant reductions of the model structural responses to gust with stability and robustness.

7 REFERENCES

- [1] Clean Sky Website, <http://www.cleansky.eu/content/page/sfwa-smart-fixed-wing-aircraft>
- [2] Tang D.M. et al., Experiments and Analysis for a gust generator in a wind tunnel, *Journal of Aircraft*, Vol. 33, N°1, Jan-Fev 1996
- [3] Ricci S. and A. Scotti A., *Wind Tunnel Testing of an Active Controlled Wing under Gust Excitation*, 49th AIAA/ASME/ASCE/AHS/ASC Structures, Structural Dynamics and Material Conference, Schaumburg, IL, USA, April 7-10 2008
- [4] Silva W.A. et al., Development of Aeroservoelastic Analytical Models and Gust Load Alleviation Control Laws of a SensorCraft Wind-Tunnel Model Using Measured Data, *IFASD 2007, International Forum on Aeroelasticity and Structural Dynamics*, Stockholm, Sweden, June 18-20 2007
- [5] Mai H. et al., Gust Response : a validation experiment and preliminary numerical simulations, *IFASD 2011, International Forum of Aeroelasticity and Structural Dynamics*, Paris, France, June 26-30 2011
- [6] Bur R., Brion V. and Molton P., An overview of recent experimental studies conducted in Onera S3Ch transonic wind tunnel, *29th Congress of the International Council of the Aeronautical Sciences (ICAS)*, St. Petersburg, Russia, September 7-12 2014
- [7] Call Fiche of Clean Sky Call for Proposal # Batch 7, http://ec.europa.eu/research/participants/portal/doc/call/fp7/sp1-jti-cs-2010-05/30842-ct-201007-v02_en.pdf
- [8] Brion V. and al., Generation of vertical gusts in a transonic wind tunnel, Submitted in Experiments in Fluids, Reviewing in progress
- [9] Huvelin F. et al., "High fidelity numerical simulations for gust response analysis, *IFASD 2013 International Forum on Aeroelasticity & Structural Dynamics*, Bristol, UK, June 24-26 2013
- [10] Rodde A.M. and Archambaud J.P., OAT15A Airfoil Data, *AGARD ADVISORY REPORT N° 303* : " A selection of Experimental Test Cases for the Validation of CFD Codes"
- [11] Farmer M.G., A two-degree of freedom mount system with low damping for testing rigid wings at different angles of attack, *NASA-TM-83302 Langley Research Center*, 1982
- [12] Bennett R. M. et al., The Benchmark Aeroelastic Models Program – Description and Highlights of Initial Results, *AGARD CP 507, Paper No. 25 in Transonic Unsteady Aerodynamics and Aeroelasticity*, 1992